Upgrading VIMOS — Part II

Peter Hammersley[1]
Ronald Brast[1]
Paul Bristow[1]
Pierre Bourget[1]
Roberto Castillo[1]
Hans Dekker[1]
Michael Hilker[1]
Jean-Louis Lizon[1]
Christian Lucuix[1]
Vincenzo Mainieri[1]
Steffen Mieske[1]
Dan Popovic[1]
Claudio Reinero[1]
Marina Rejkuba[1]
Chester Rojas[1]
Ruben Sanchez-Jannsen[1]
Fernando Selman[1]
Alain Smette[1]
Josefina Urrutia Del Rio[1]
Javier Valenzuela[1]
Burkhard Wolff[1]

[1] ESO

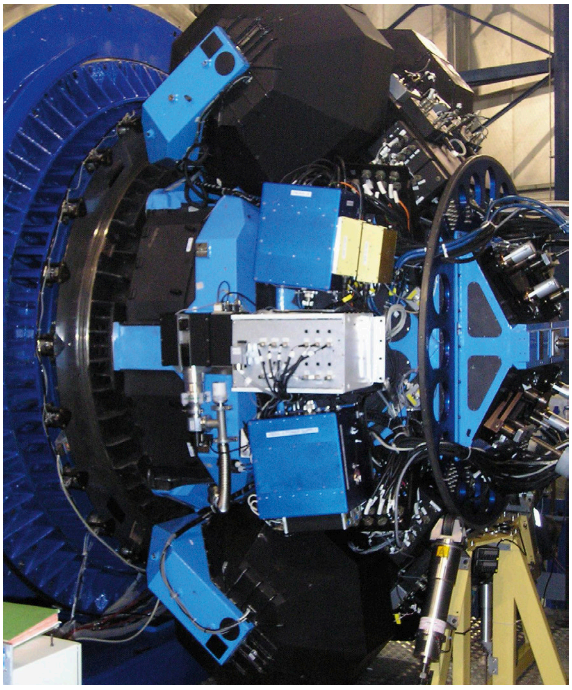

Figure 1. VIMOS on the Nasmyth platform of VLT UT3.

VIMOS is the powerful visible (360–1000 nm) imager and multi-object/integral field spectrometer mounted on the VLT Unit Telescope 3, Melipal. Its high multiplex advantage makes it ideal for undertaking large-scale spectroscopic surveys of faint sources. In order to extend the life of the instrument, improve its performance and prepare for possible large-scale surveys, in 2009 it was decided to upgrade VIMOS. The first phase of the upgrade, which included replacing the detectors and the fitting of an active flexure compensation system, has been previously reported; this article describes the second stage of the upgrade, which has improved the delivered image quality and stability.

The instrument and upgrades

VIMOS has four identical arms, each with a 7 by 8 arcminute field of view on the sky with a gap between the fields of 2 arcminutes. The instrument offers three main modes:
- *UVBRIz*-band imaging covering four fields each 7 × 8 arc-minutes;
- slitlet-based multi-object spectroscopy with spectral resolutions from a few hundred to 2500 in each of the four imaging fields;
- integral field unit (IFU) spectroscopy with three fields of view: 13 by 13, 27 by 27, and 54 by 54 arcseconds depending on the specific mode requested.

VIMOS and its commissioning on the VLT in 2002 were described in Le Fevre et al. (2002) and in operation by D'Odorico et al. (2003). After eight years of operation it became necessary to upgrade the instrument in order to address various issues and to extend its useful life. The first phase of the upgrade was implemented in 2010, (Hammersley et al., 2010) and included:
- Replacement of the shutters, which were worn out.
- Replacement of the CCD detectors, which has improved the sensitivity in the red and reduced the fringing.
- Reduction of the instrument flexure.
- Provision of new mask cabinets that keep masks in position more reliably.
- Improvement of the data reduction pipeline.

The second upgrade phase took place in 2011–12 and addressed a number of issues which became apparent following the first phase: image quality; the focus mechanisms and their control; the efficiency of the HR-blue grism; calibration and operational procedures; and operational efficiency.

This article discusses the results of this second phase. More technical details on the overall upgrade programme can be found in Hammersley et al. (2012).

Improving image quality

Following the change of the detector, it became apparent that the optimum focus was changing across the detector due to a tilt between the detector and the re-imaged focal plane. This meant that if the detector was well focused at its centre, then the edges would not be as well focused. Due to the optical configuration of VIMOS this could lead to the images at the corners of each detector becoming significantly elongated.

In May 2011 an intervention was made to correct this effect by moving one of the lenses and the detector laterally with respect to the rest of the optics. This reduced the tilt between the telescope focal plane and detector by typically a factor five. At the correct focus only the extreme corners of the array showed a small amount of astigmatism. Figure 2 shows the evolution of average

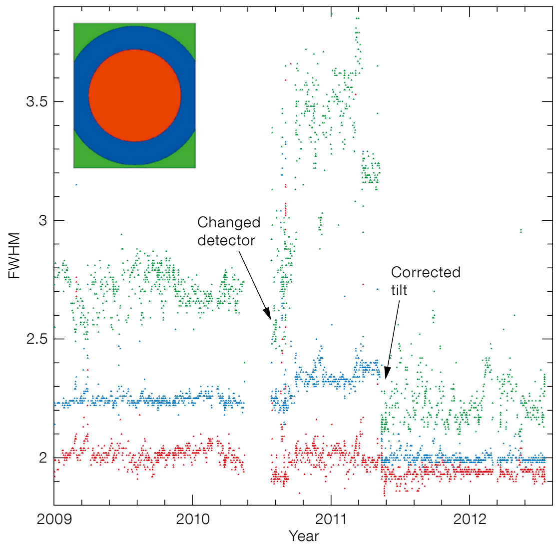

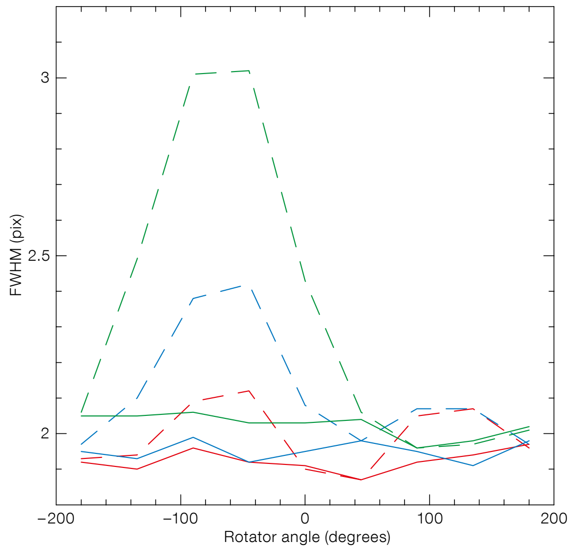

Figure 3. Variation of the FWHM in pixels with rotator angle for VIMOS channel 3. The dashed lines show the case with no focus compensation and the solid lines with compensation.

Figure 2. Evolution of the image FWHM in pixels since 1 January 2009 for VIMOS channel 4. The red points correspond to the average FWHM of the pinholes within 800 pixels of the centre; blue between 800 and 1200 pixels and green to those beyond 1200 pixels (see the schematic of the regions used on the detector to the upper left). Arrows mark when the detector was changed and the tilt corrected.

image quality in three regions of detector 4 since 1 January 2009. The data were obtained using daytime calibration images of a pinhole mask placed in the focal plane. The dates when the detector was changed and the tilt corrected are marked with arrows on Figure 2. The degradation of image quality following the detector exchange is clear, but following the correction of the tilt, the image quality towards the edge of the detector has significantly improved. Currently, approximately 90 % of the imaging area has an image full width at half maximum (FWHM) < 2.4 pixels and an ellipticity below 0.1, whereas prior to the upgrade it was closer to 70 %.

Focus control

The original focus mechanism and control software also limited the performance of the instrument. Among the problems were: the stepper motor could lose steps and so lead to a drift in the focus position of the camera; the camera focus changed significantly with the rotator angle and this could not be corrected; it was not possible to control the focus for each grism; updating the focus parameters in the control software was very complicated and it was very easy to inadvertently make mistakes which were not immediately obvious.

In March 2012 the original focus stepper motors were replaced with DC motors, each with an encoder. The software was updated to allow the focus offset to now take into account rotator angle and grism as well as temperature and filter for each channel. After implementing the new motors and encoders, it was found that the mechanism did not have sufficient range to focus all of the modes correctly, affecting in particular the IFU, and so a further intervention in October 2012 was required to correct this.

Figure 3 shows the variation in FWHM with rotator angle when observing the pinhole mask for the three colour-coded regions designated in Figure 2. The dashed lines show the FWHM with no compensation with rotator angle and the solid lines indicate the cases with compensation. This plot demonstrates that the instrument is now far closer to the optimum focus in normal operation where the rotator angle is constantly changing.

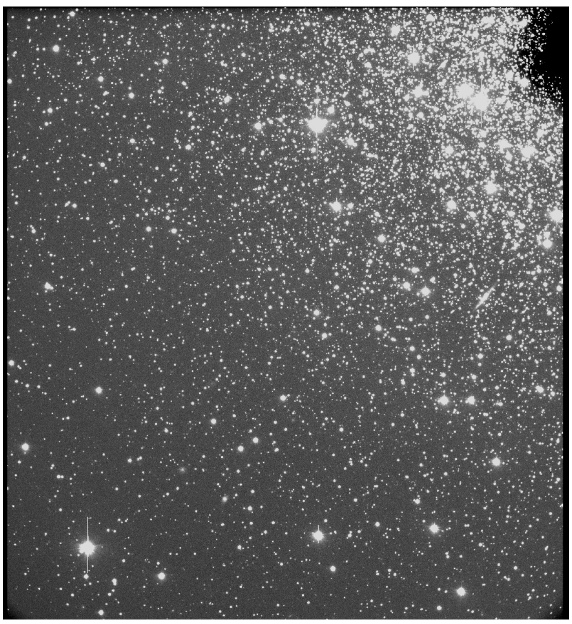

Figure 4. *R*-band image of the globular cluster M55 taken in October 2012, after the focus upgrade. This shows the whole field of view in channel 3 (7 by 8 arcminutes). The dark area to the top right is caused by the guide probe vignetting the image.

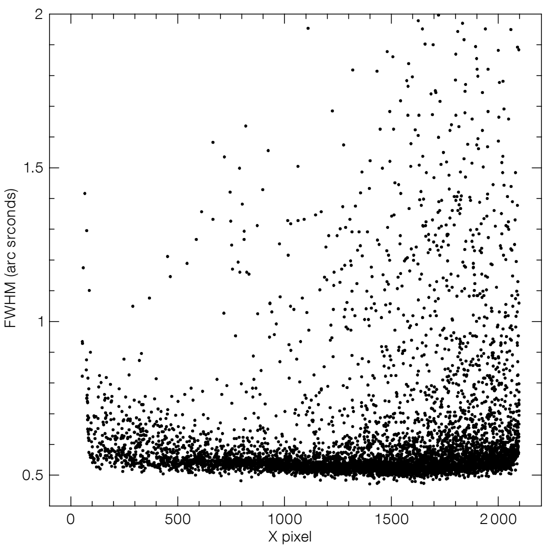

Figure 5. The variation of the stellar FWHM, in arcseconds, as a function of the X position on the image shown in Figure 4.

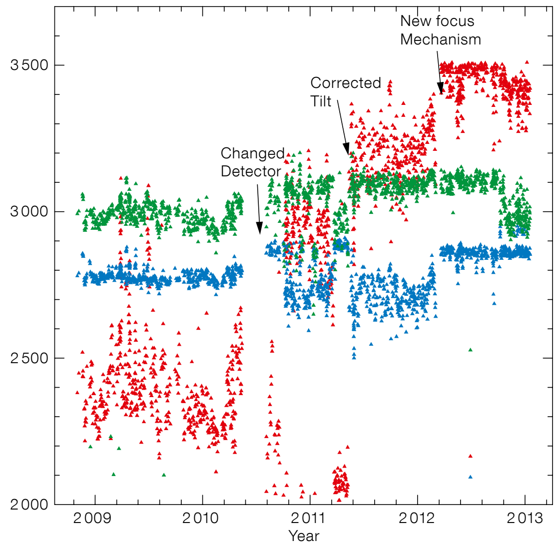

Figure 6. The spectral resolution in the red, blue and central regions of lamp spectra, colour-coded red, blue and green, taken with the HR-orange grism in IFU mode for channel 1 is shown. The dates when the detector was changed, the tilt corrected and the new focus mechanism were implemented are all marked. It should be noted that this is one of the more extreme examples.

Figure 4 shows a VIMOS *R*-band image of the globular cluster M55, taken with 0.5-arcsecond seeing during the last intervention. This uses the full imaging field of view on channel 3. Figure 5 shows how the image quality varies with position on the horizontal axis (X direction). The sources with FWHM ~ 0.55 arcseconds are stars, while extended background objects and blended stars have larger FWHM, in particular near the centre of the globular cluster (top right). There is some elongation in the bottom corners of the image and the FWHM in those regions increases from about 0.55 to 0.60 arcseconds.

Spectral resolution

The grisms used by VIMOS are placed in the pupil and it was originally assumed that these would not significantly affect the focus. Tests in May 2011, however, showed that this was not the case, and the high-resolution grisms in particular required a significant focus offset if the spectral resolution was to be maintained across the whole detector. When the focus was not optimum then the resolution was degraded, particularly at each end of the spectral range. The new focus control allows the focus to be set for each grism and this has led to the resolution being more uniform between the four quadrants and over time. The red end of the spectrum now always has a higher resolution than the blue (as it should be), which was not always the case beforehand.

As an illustration of the implication of this change for observations, we estimate that programmes to detect Lyman-α emitters at high redshift would have up to a 40% gain in sensitivity just because the red end of the HR-red spectrum

Figure 7. The total VIMOS efficiency when using the old (purple) and new (green) HR-blue grisms is shown.

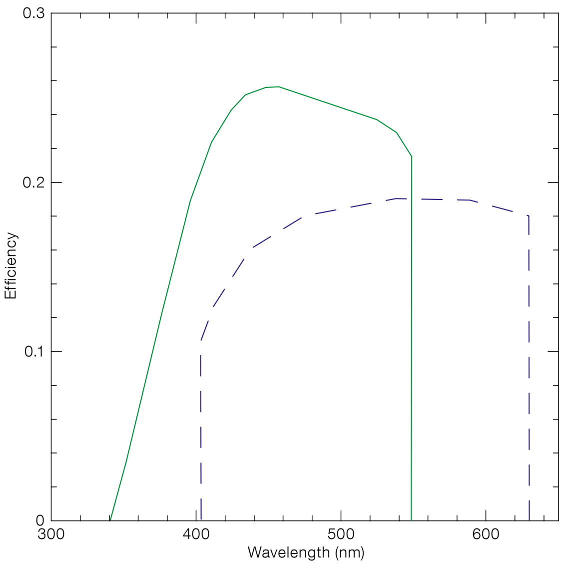

Figure 8. The evolution of the average technical down time of VIMOS from 2008 to 2011 showing the improvement resulting from the upgrade activities.

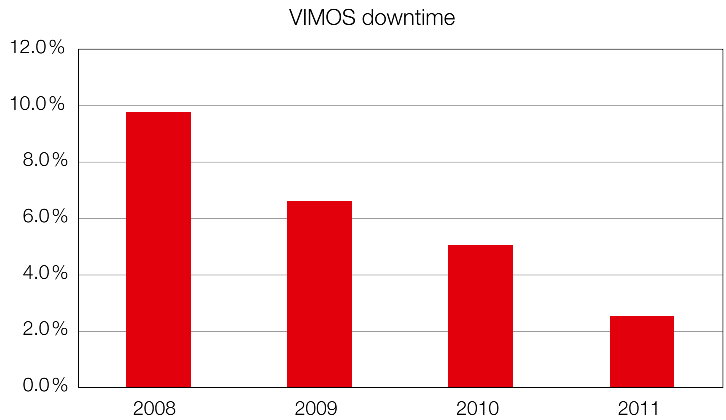

is now in focus. Figure 6 shows the evolution of the resolution of the HR-orange grism for channel 1 since 2009. The dates when the detector was changed, the tilt corrected and the new focus mechanism installed are marked. As is apparent, since March 2012 the red spectral region, in particular, has improved, although some fine tuning is still required.

HR-blue grism

The original HR-blue grism had a relatively low transmission and so early on when the upgrade was planned it was decided to replace it with a Volume Phase Holographic (VPH) grism. The transmission of the new grism is up to about 50% higher and there is useful transmission below 360 nm (Figure 7). The spectral resolution has, however, been reduced by about 30% and the new dispersion is 0.71 Å per pixel.

Operations

A significant effort has been made to improve the reliability of VIMOS. Some of the maintenance procedures have been modified and strengthened, such as making a test insertion every time a new mask is loaded into the instrument. As Figure 8 demonstrates, these procedures have noticeably reduced the technical down time.

Additional steps have also been taken to make the science operations more efficient. One example is the elimination of the mandatory need for pre-imaging using the PILMOS mode to prepare the masks, which can now be cut directly, based on user catalogues (see Bristow et al., 2012).

An upgraded VIMOS

The VIMOS upgrade programme, which is now nearing its conclusion, has been made possible by a significant and successful collaboration between the ESO staff at Garching and Paranal. The most important improvements are:
1) The instrument has a better sensitivity in the red.
2) There is far lower detector fringing, allowing better sky subtraction in the red.
3) Opto-mechanically, VIMOS is more stable, which makes the instrument simpler to calibrate.
4) There is a higher and more stable image quality across the whole detector.
5) The observing efficiency has improved.
6) The technical down time has decreased.

As a result, VIMOS is now a significantly more powerful instrument that when it was originally mounted on the telescope and it is ready for many more years of ground-breaking science.

References

Bristow, P. et al. 2012, The Messenger, 148, 13
D'Odorico, S. et al. 2003, The Messenger, 113, 26
Hammersley, P. et al. 2010, The Messenger, 142, 13
Hammersley, P. et al. 2012, SPIE, 486, 5MH
Le Fevre, O. et al. 2002, The Messenger, 109, 21

ESO/R. Gendler

VIMOS colour image of the barred spiral galaxy NGC 1097, with additional colour information from an image taken by amateur astronomer Robert Gendler superimposed. VIMOS images in *B*-, *V*- and *R*-bands were combined and highlight the star formation regions in the spiral arms, the dust lanes in the bar and the starburst ring around the active galactic nucleus. The companion elliptical galaxy is NGC 1097A at a similar distance of 20 Mpc. See Picture of the Week 11 July 2011 (potw1128a) for more details.